Random Bragg-gratings-based narrow linewidth random fiber laser with a π-phase-shifted FBG

Shuaijie Miao (苗帅杰)[1,2], Wentao Zhang (张文涛)[2,*], and Ying Song (宋 颖)[1]

[1]*School of Traffic and Transportation, Shijiazhuang Tiedao University, Shijiazhuang 050043, China*
[2]*Optoelectronic System Laboratory, Institute of Semiconductors, Chinese Academy of Sciences, Beijing 100083, China*
**Corresponding author: zhangwt@semi.ac.cn*

Received May 2, 2019; accepted June 4, 2019; posted online August 12, 2019

A new structure of short-cavity random fiber laser (RFL) with narrow linewidth lasing is proposed. A π-phase-shifted fiber Bragg grating (FBG) loop mirror was used in the RFL for spectral filtering and to suppress multi-mode oscillation due to the narrow transmission window. The random feedback of the RFL was implemented by a randomly dispersed weak reflection FBG array. The high gain of the erbium-doped fiber and a half-open cavity design results in a low lasing threshold. The linewidth of the laser was 225 Hz with 58 dB side-mode-suppression ratio. The laser threshold was 4.5 mW, and the optical signal-to-noise ratio was up to 63 dB.

OCIS codes: 060.3735, 060.2370.
doi: 10.3788/COL201917.090605.

The linewidth of a laser source is critical in high-resolution optical fiber sensing systems due to its contribution to noise level suppression[1–5]. Random fiber lasers (RFLs) have a compact structure, low lasing threshold, and good temporal coherence and, thus, are a promising choice for different types of narrow linewidth lasers[6,7].

Most previous random feedback devices in RFLs are based on distributed feedback of Rayleigh backscattering (RBS), using tens of kilometers of single-mode fiber (SMF). Single-mode narrow lasing on the order of several hertz to several hundred hertz can be established in RBS-based RFLs with a low pump threshold based on stimulated Brillouin gain combined with optical filters[8,9]. It is noteworthy that due to the extremely weak RBS coefficients, providing effective mode suppression and random distributed feedback often requires up to tens of kilometers of SMFs. Moreover, the coupling and intense competition of high-density random modes in long SMFs lead to obvious frequency jitter, reducing the laser stability[10].

RFLs with a short-cavity structure have been widely investigated due to their narrow linewidth and low lasing threshold[11]. Random feedback of this type of RFLs is realized by short (tens of millimeters to several meters) random distributed feedback fiber (RDFF), which can be formed by a variety of high-precision fiber Bragg grating (FBG) configurations with random intervals, such as randomly spaced FBG array[12], multi-phase-shifted FBGs[13], randomly spaced chirped gratings, and random refractive index modulation surfaces. Thus, these RFLs have a simpler structure and are less affected by environmental turbulence. Different from the RBS random feedback mechanism, on one hand, random gratings strongly improve the random feedback efficiency and have wavelength dependence by introducing refractive index modulation. Moreover, combining the high-efficiency gain provided by short active fibers and a half-open cavity can result in a low lasing threshold[14]. On the other hand, the RDFF can be regarded as the superposition of many Fabry–Pérot interferometers (FPIs) to filter out some random modes. Increasing randomness is beneficial to a narrow linewidth[15]. However, the number of FBGs written in RDFF is not infinite, which limits RFLs to achieve higher randomness, and the random inhomogeneity introduced by external refractive index modulation limits the further compression of laser linewidth. In addition, the mode competition caused by the energy disturbance in resonators leads to poor wavelength stability. Various spectral filter components and mode-locking techniques, such as fiber FPI filters[16], dynamic particle number inversion gratings[17], and bandpass filters, have been proposed in RFLs to further narrow the output for single-mode coherent operation and improve time-domain stability. In addition to the optical filters mentioned above, the optical filtering characteristics of a π-phase-shifted FBG (π–FBG) have been confirmed in conventional fixed-cavity fiber lasers[18]. However, the configuration of combining an RDFF and a π–FBG in a short-cavity RFL to achieve narrow linewidth laser output has not been reported, and the laser linewidth for short-cavity RFLs was still maintained at a kilohertz (kHz) magnitude[19,20].

In this Letter, a new structure of short-cavity RFL with a π–FBG loop mirror is proposed, which leads to a 225 Hz narrow lasing linewidth. Random feedback in the RFL is provided by an RDFF consisting of a weak FBG array, and the internal random Fabry–Perot (FP) resonator effect guides the oscillation of particular random resonant modes. A π–FBG loop mirror is used in the RFL for reducing the number of random lasing modes and spectral filtering to ensure a further stable narrow linewidth output. The high gain of erbium-doped fiber (EDF) combines with a half-open cavity consisting of a ring fiber and weak

FBGs to achieve a low lasing threshold. To the best of our knowledge, it is the first time that a π–FBG loop mirror is used in a short-cavity RFL and realizes a sub-kHz narrow linewidth laser.

The experimental setup of the proposed RFL system is shown in Fig. 1. A 0.4 m EDF (Er110-4/125, Liekki) is pumped by a 980 nm laser diode via a 980/1550 nm wavelength division multiplexer (WDM) to establish an efficient gain spectrum. The RDFF consists of 20 weak Bragg gratings written at random spacing along the axial direction of an SMF (Corning-28) with a total length of 164.5 mm. The FBGs are etched on fiber through a phase mask and UV exposing technique. Gratings are effective scattering elements, and the randomness introduced by random spacing forms many disordered local cavities in a grating array, which restricts the multiple scattering of light and leads to light localization[21], thus realizing the random feedback. The randomly spaced weak FBGs increase the effective length of the laser cavity and improve the frequency selection[12]. The Bragg wavelength and reflectivity of each 3 mm FBG are 1537.480 nm and ~4%, respectively. The separation between two FBGs was chosen arbitrarily in the range of 3–8 mm, as shown in Fig. 2. The 1550 nm port of the WDM connects the ring optical path, consisting of an optical circulator and a π–FBG. The circulator maintains the unidirectional transmission of light and can suppress the spatial hole burning effect. This high-reflectivity ring optical mirror and weak grating array constitute a half-open cavity structure, which can significantly reduce the lasing threshold. A π–FBG, which has a transmission linewidth of about 13.7 MHz, is formed by introducing a π phase shift into the center of a 5.8 cm FBG structure, and the reflection bandwidth of the π–FBG covers the spectral envelope of the highly dispersed reflectors in RDFF for spectral filtering. The isolator at the laser output end ensures that the feedback is only caused by the RDFF. Lasing behavior occurs when the gain exceeds the loss in resonators. The laser spectrum and power are monitored by an optical spectrum analyzer (AQ6370 C, Yokogawa) and a power meter (OLP-6, Acterna).

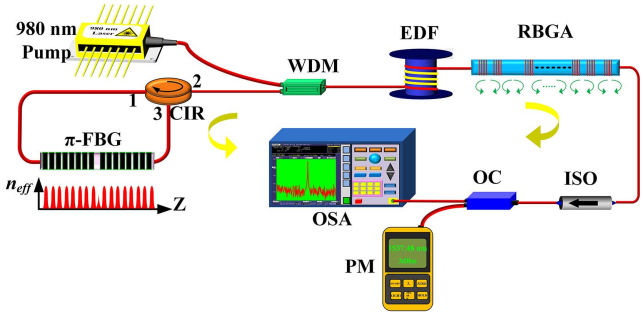

Fig. 1. Experimental setup of the RFL. RBGA, random Bragg grating array; OSA, optical spectrum analyzer; PM, power meter; CIR, circulator; OC, optical coupler; ISO, isolator.

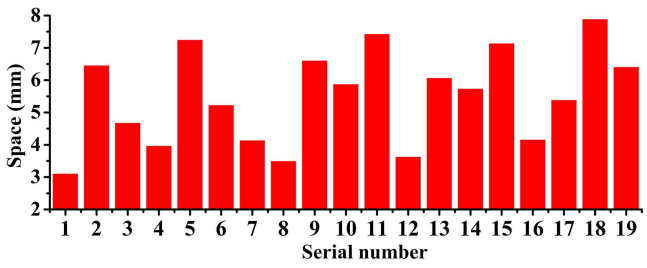

Fig. 2. Detailed random spacing along the fiber during the RDFF fabrication process.

Figure 3 shows the reflection and transmission spectra of the RDFF. The results indicated a relatively wide reflectance spectrum with a center of 1537.48 nm and a 3 dB bandwidth of 0.35 nm. The deviation from the wavelength and reflectance of the FBGs was caused by recording bias, hydrogen leakage, and temperature fluctuation. Narrow peaks caused by interference between different FBG pairs can be observed in the spectrum. To some extent, the RDFF can be viewed as an optical filter superposed on many randomly distributed narrow-band FPIs that allows some special (resonant) wavelengths to pass through. It is slightly different from the short-cavity RFLs, in which weak gratings are etched on doped fiber[22]; the separation configuration of the random distributed feedback and gain reduce the thermal disturbance in RDFF and improve the stability of the laser to a certain extent[23].

The trend of RFL output power as a function of pump power is shown in Fig. 4. The upper inset of Fig. 4 shows a typical laser threshold behavior at 4.5 mW, which is one order of magnitude lower than previously suggested configurations[22,24]. Such a low lasing threshold can be attributed to the design of the half-open cavity and the use of high-gain EDFs. When the pump exceeds the threshold, the output power increases linearly with increasing pump power with a linearity of up to 99.49%, and the calculated slope efficiency is 1.83%. The output power was 3.49 mW at a pump power of 200 mW.

Figure 5 shows variations in the output spectrum with changes in the pump power. Random resonator modes

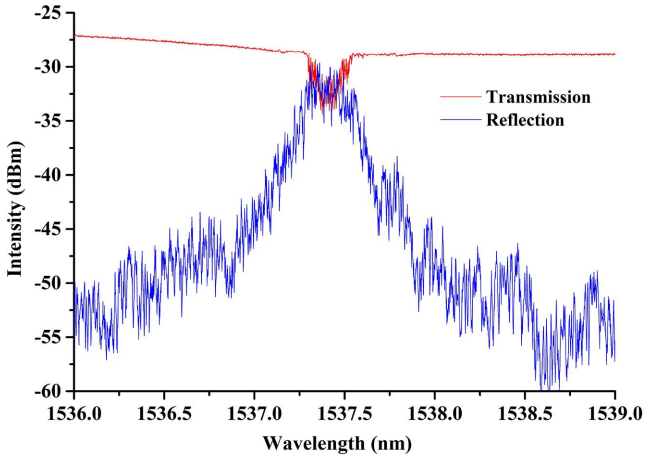

Fig. 3. Reflection and transmission spectra of the RDFF.

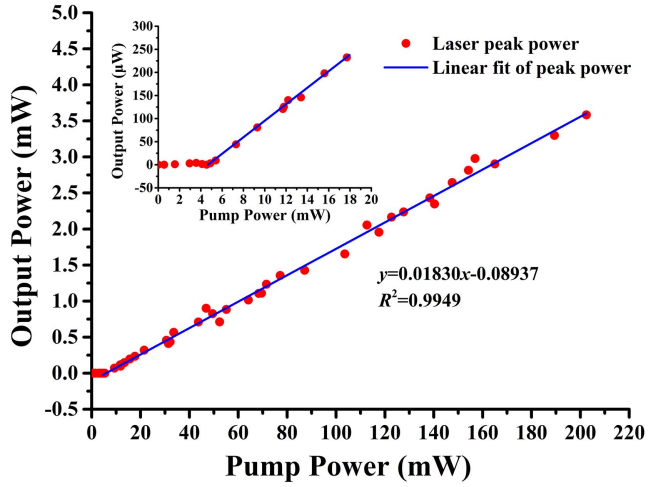

Fig. 4. Output power of the RFL versus pump power. The upper inset shows an enlargement of the output-input curve near the threshold.

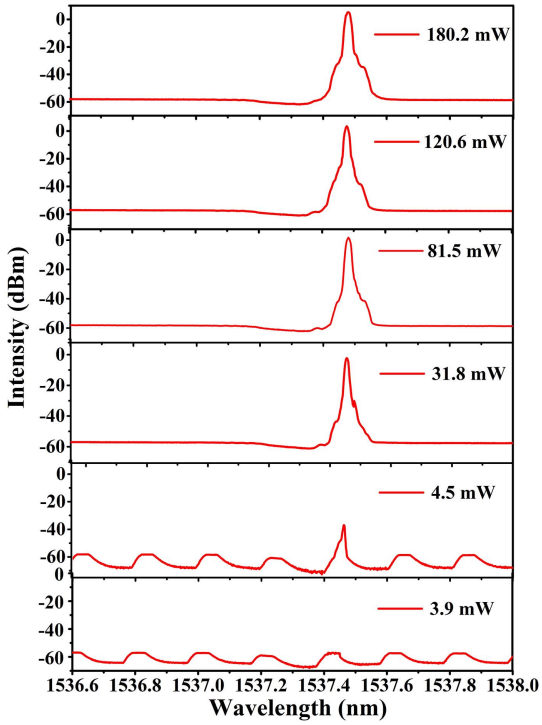

Fig. 5. Changes in the output spectrum of the RFL with in the pump power.

generated within the proposed RFL are related to two oscillating regimes, which are represented by green and yellow arrows in Fig. 1, respectively. Regime I is formed between FBGs, and regime II is between one of the FBGs and the ring mirror. When the pump power is near the threshold, the emitted modes are unstable and have chaotic characteristics, and the spectrum is formed by regimes I and II. With increasing pump power, more random subcavity modes appear in the narrow transmission region of the π–FBG, mainly due to the resonators of regime I[14]. According to the results, a single-mode lasing operation near 1537.479 nm is maintained. The laser spectra show an optical signal-to-noise ratio (OSNR) of up to 63 dB at a pump power of 180.2 mW.

The curves in Fig. 6 show the time-varying output spectra of the RFL with and without the π–FBG at pump power of 200 mW. As shown by the spectral lines of different colors in Fig. 5(a), with time, almost no single stable narrow linewidth lasing behavior occurs without a π–FBG. The wide and random splitting laser spectra in Fig. 6(a) can be regarded as the collection of the localized spatial modes with different slope efficiencies and threshold power in the array[25]. The lasing modes are determined by many superimposed random FP filters with low reflection coefficients along the RDFF. High pump power induces more resonant modes, causing low quality factors in the RDFF to be emitted and locked, resulting in spectral broadening. The spectrum fluctuates randomly with time due to mode hopping, which is exacerbated by broadband linear gain and fluctuations of energy in random cavities. In addition, nonlinear effects and

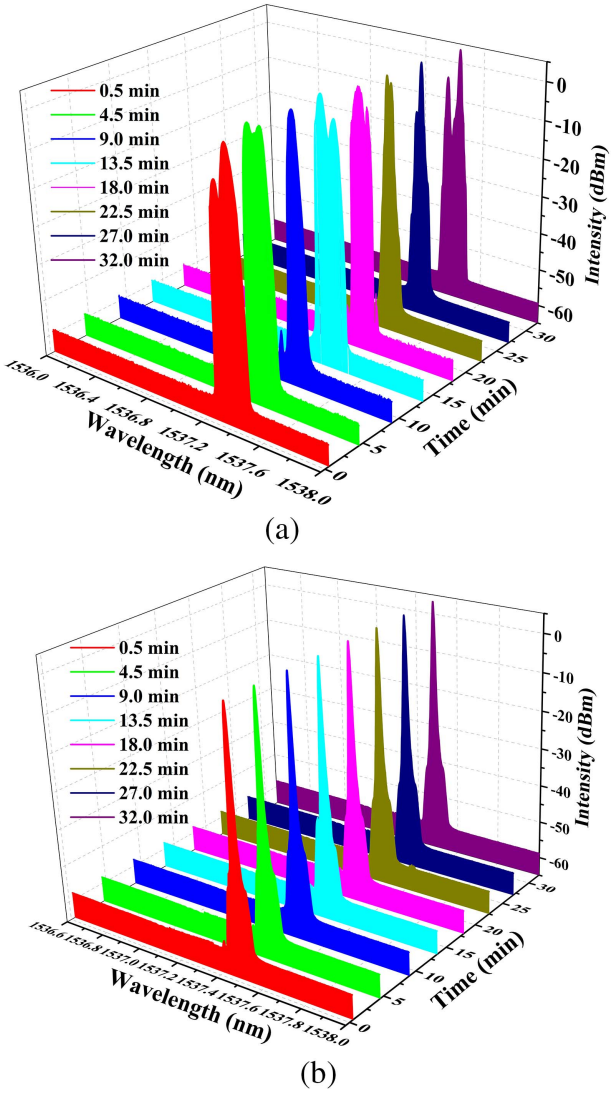

Fig. 6. Time-stability test results of emission spectra of the proposed RFL (a) without a π–FBG and (b) with a π–FBG.

non-uniform distribution of light intensity in optical fibers also cause the fluctuation of the lasing spectrum at high pump power.

Figure 6(b) shows that when a π–FBG is included in the RFL, a narrow single-wavelength laser with slight fluctuations in the spectrum is achieved in 30 min. The π–FBG only accommodates limited narrow spectral filters in the RDFF and suppresses most oscillation modes. The random feedback of the resonant frequencies corresponding to the transmission window is enhanced. The dominant position in the mode competition is consolidated[26], leading to a stable narrow linewidth coherent output.

Figure 7 shows the variation of wavelength and output power in 20 min at 40, 80, and 153 mW. The laser was placed in an acoustic chamber to reduce external interference. The figure shows that the lasing wavelength and power exhibit relative stability. The π–FBG in the RFL adjusts the transmission loss of random cavities and effectively reduces the amount of resonant modes. The lasing frequency is locked in the narrow transmission windows, ensuring a relatively stable laser wavelength. The high stability of the pump light and a small number of resonant modes contribute to the time-domain stability of the output power. The maximum fluctuation range of the output wavelength is ~3.1 pm. The disturbance of external heat and low frequency vibration to π–FBG with time causes its Bragg wavelength shift, thus leading to the fluctuation of laser frequency. In addition, the existence of mode competition in a narrow transmission window also contributes to the shift of the laser wavelength. The tendency to drift toward a long wavelength can be observed at different pump powers. The slight blue shift of the wavelength with time is attributed to the increase of core temperature in the π–FBG and RDFF, due to light oscillation and transmission in random cavities[27]. The stability of the laser wavelength and output power may be further improved by introducing random phase shifts into this RDFF or attempting the saturated absorber technology.

We used a commercial lead zirconate titanate (PZT) tunable fiber laser (NKTE15, linewidth less than 100 Hz) and the RFL to measure lasing linewidth through optical heterodyne beat frequency[28]. The output powers of the RFL and the narrow NKT fiber laser were kept near approximate with a variable optical attenuator. The wavelength of the random laser was collected by a spectrograph with a wavelength resolution of 0.04 pm, and the beat of the NKT fiber laser of around 1537.4 nm was determined by a coupler and a high-speed photoelectric detector (KG-PR-200M-A, Conquer). Then, an oscilloscope can record the beat frequency laser linewidth. In the experiment, an NI FlexRIO apparatus (NI 7966 R FPGA module and NI 5734 A/D board) and LabVIEW software were used to build the oscillating system. The data sampling rate of the NI 5734 was set to 120 MHz, and the data length for the linewidth computation was ~0.04 s (corresponding to 5,000,000 sampling points). According to Nyquist functions, the frequency resolution of the oscilloscope was 12 Hz.

Figure 8 shows the beat signal of the RFL and NKT fiber laser. The linewidth of beat frequency obtained in the experiment was about 6.49 kHz at 20 dB, corresponding to a Lorentz linewidth of 3 dB at ~325 Hz, which shows that the linewidth of the photocurrent was about the sum of the two independent lasers. The laser linewidth of the RFL can be calculated to be about 225 Hz, and the side-mode-suppression ratio (SMSR) was about 57 dB.

In summary, we proposed a novel structure of a short-cavity-based RFL for a narrow linewidth random coherent optical operation. The use of a π–FBG loop mirror further limits the number of sub-cavity modes of oscillation and locks the lasing peak, which effectively ensures a stable and narrow lasing operation. A linewidth of 225 Hz and an SMSR of 57 dB have been achieved. The design of the half-open cavity combined with a high-gain EDF was used to significantly improve the random feedback efficiency and resonator quality factor. A low lasing

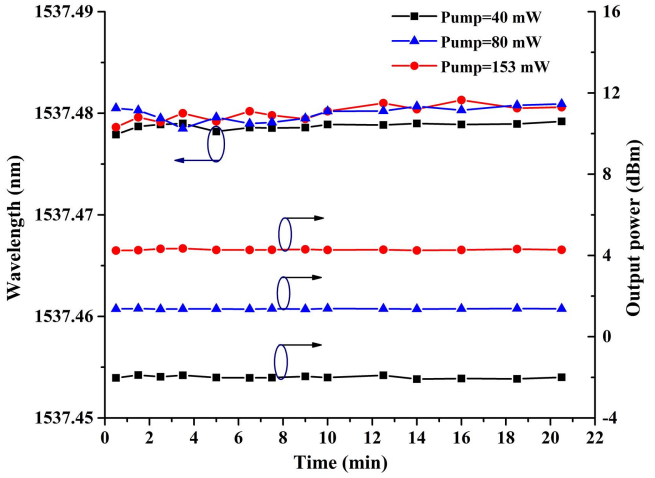

Fig. 7. Stability of emission wavelength and output power with time at 40, 80, and 153 mW pump power.

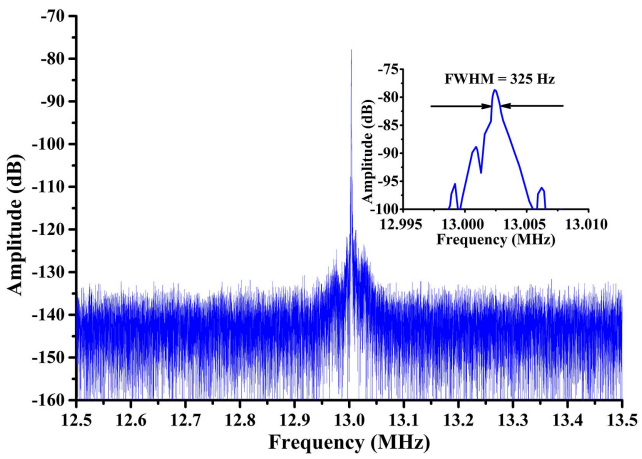

Fig. 8. Detection signal of the laser beat linewidth based on an optical heterodyne.

threshold of 4.5 mW was obtained. After exceeding the lasing threshold, the output spectra exhibited relatively good wavelength and power stability. An OSNR of up to 63 dB was obtained near 1537.479 nm. This is the first time , to the best of our knowledge, to filter in a short-cavity-based RFL using a π–FBG loop mirror and obtain sub-kHz linewidth laser output. The RFL with its simple configuration has a small size and low lasing threshold and can stably launch a single-mode narrow coherent lasing operation, which provides a new option for high-resolution optical sensing and coherent communication.

This work was supported by the National Key R&D Program of China (No. 2017YFB0405503), the Youth Innovation Promotion Association of CAS (No. 2016106), the National Natural Science Foundation of China (No. 61875185), and the Innovation Project of Shijiazhuang Tiedao University (No. YC2019049).

References

1. X. Huang, Q. Zhao, W. Lin, C. Li, C. Yang, S. Mo, Z. Feng, H. Deng, Z. Yang, and S. Xu, Opt. Express **24**, 18907 (2016).
2. W. Zhang, F. Zhang, F. Li, and Y. Liu, Proc. SPIE **7503**, 126 (2009).
3. Z. Shen, L. Wang, Y. Cao, X. Wang, X. Feng, and B.-O. Guan, Chin. Opt. Lett. **15**, 100601 (2017).
4. Y. Zhang, C. Gao, Q. Wang, Q. Na, M. Zhang, M. Gao, and S. Huang, Chin. Opt. Lett. **17**, 031402 (2019).
5. T. Yang, Y. Song, W. Zhang, and F. Li, Chin. Opt. Lett. **14**, 120602 (2016).
6. M. Gagné and R. Kashyap, Opt. Lett. **39**, 2755 (2014).
7. J. Xu, J. Ye, H. Xiao, J. Leng, J. Wu, H. Zhang, and P. Zhou, Opt. Express **24**, 19203 (2016).
8. P. Meng, B. Xiaoyi, and C. Liang, Opt. Lett. **38**, 778 (2013).
9. Y. Xu, D. Xiang, Z. Ou, P. Lu, and X. Bao, Opt. Lett. **40**, 1920 (2015).
10. B. Saxena, X. Bao, and L. Chen, Opt. Lett. **39**, 1038 (2014).
11. Z. Guo, J. Song, Y. Liu, Z. Liu, S. Ping, and X. Dong, Appl. Phys. B **124**, 48 (2018).
12. N. Lizárraga, N. P. Puente, E. I. Chaikina, T. A. Leskova, and E. R. Méndez, Opt. Express **17**, 395 (2009).
13. L. Wang, X. Dong, P. P. Shum, X. Liu, and H. Su, J. Lightwave Technol. **33**, 95 (2014).
14. W. L. Zhang, Y. J. Rao, J. M. Zhu, Z. X. Y. Z. N. Wang, and X. H. Jia, Opt. Express **20**, 14400 (2012).
15. M. Gagné and R. Kashyap, Opt. Express **17**, 19067 (2009).
16. S. Srikanth, T. Nikita, S. Xuewen, and D. V. Churkin, Opt. Express **21**, 16466 (2013).
17. S. M. Popov, O. V. Butov, Y. K. Chamorovski, V. A. Isaev, P. Mégret, D. A. Korobko, I. O. Zolotovskii, and A. A. Fotiadi, Results Phys. **9**, 806 (2018).
18. Y. Zhao, J. Chang, Q. Wang, J. Ni, Z. Song, H. Qi, C. Wang, P. Wang, L. Gao, Z. Sun, G. Lv, T. Liu, and G. Peng, Opt. Express **21**, 22515 (2013).
19. Y. Li, P. Lu, X. Bao, and Z. Ou, Opt. Lett. **39**, 2294 (2014).
20. L. Yang, L. Ping, F. Baset, Z. Ou, S. Jia, A. Alshehri, V. R. Bhardwaj, and X. Bao, Appl. Phys. Lett. **105**, 558 (2014).
21. O. Shapira and B. Fischer, J. Opt. Soc. Am. B **22**, 2542 (2005).
22. L. Wang, X. Dong, P. P. Shum, X. Liu, and H. Su, J. Lightwave Technol. **33**, 95 (2015).
23. A. Zhang and L. Hao, Appl. Opt. **57**, 10017 (2018).
24. X. Wang, D. Chen, H. Li, L. She, and Q. Wu, Appl. Opt. **57**, 258 (2018).
25. A. Fotiadi, Nat. Photon. **4**, 204 (2010).
26. F. N. Timofeev and R. Kashyap, Opt. Express **11**, 515 (2003).
27. E. Rønnekleiv, Opt. Fiber Technol. Mater. Devices Syst. **7**, 206 (2001).
28. K. M. Abramski, W. Rodzen, P. R. Kaczmarek, L. Czurak, and A. Budnicki, in *Proceedings of 2003 5th International Conference on Transparent Optical Networks* (2003), p. 87.